DOE/ER/40617-129

VACUUM STRUCTURE OF PURE GAUGE THEORIES ON THE LATTICE[1]

DOE/ER/40617--129

DE93 001920

Richard W. Haymaker, Vandana Singh and Dana Browne
Department of Physics and Astronomy
Louisiana State University, Baton Rouge, Louisiana, 70808, USA

and

Jacek Wosiek
Chair of Computer Science
Jagellonian University, Institute of Physics, Reymonta 4 Cracow, Poland; and
Max-Planck-Institut für Physik - Werner-Heisenberg-Institute - P.O. Box 40 12 12, Munich, Germany

ABSTRACT

We present results from simulations on two aspects of quark confinement in the pure gauge sector. First is the calculation of the profile of the flux tube connecting a static $q\bar{q}$ pair in $SU(2)$. By using the Michael sum rules as a constraint we give evidence that the energy density at the center of the flux tube goes to a constant as a function of quark separation. Slow variation of the width and energy density is not ruled out. Secondly in the confined phase of lattice $U(1)$ we calculate the curl of the magnetic monopole current and show that the dual London equation is satisfied and that the electric fluxoid is quantized.

1. Introduction

I would like to report on efforts of the Cracow-LSU collaboration to study the response of gauge fields to the presence of static sources. Confinement is the central issue which is seen as a consequence of the vacuum squeezing the field lines to form flux tubes connecting color charges. One is beginning to see considerable detail of the field distributions in the flux tube, e.g. its size and shape, the chromoelectric and chromomagnetic field components, and monopole currents that are responsible for squeezing the tube to form an Abrikosov vortex.

In the first part of this talk I will describe our results for SU(2) lattice gauge theory[1,2,3]. We examine the flux tube between a $q\bar{q}$ pair, calculating the six chromoelectric and chromomagnetic components to the energy density and action density. We parametrize the profile of the flux tube and study scaling. The results are subjected to the check provided by the Michael sum rules[4].

The second part of this talk concerns the mechanism that leads to flux tube formation. This is the role of the solenoidal magnetic monopole currents that surround

[1]Talk at 1992 Paris Conference on the QCD Vacuum presented by R. Haymaker

DISCLAIMER

the flux tube. In this work[5] we show in the confined phase of U(1) that the curl of the monopole current has a profile similar to the electric field and that the dual London equation is satisfied and electric fluxoid quantization occurs. We demonstrate that the the flux tube is precisely the dual of the Abrikosov vortex in Type II superconducting materials.

2. Flux Tubes in SU(2) [2]

2.1. Background

In this calculation we measure the field energy densities by correlating the small plaquette with the Wilson loop. Full details of the simulation are given in Ref. [2], which also contains further references. Further details of the flux profiles will appear in a companion paper Ref. [3]. By fixing our attention on the middle time slice of the Wilson loop, the time-like segments form world lines that approximate a static $q\bar{q}$ pair. The 3 space-space plaquettes measure the magnetic component of the energy density and similarly the 3 space-time plaquettes measure the electric components.

Before defining the flux calculation in more detail, we point out that the Wilson loops themselves are used to extract the transfer matrix eigenvalues which give the static quark potential and are further used to extrapolate the flux measurements to infinite time extent of the Wilson loops. Specifically we determine the eigenvalues of the transfer matrix by fitting the Wilson loops to the exponentials as described in Ref.[2].

$$< W(R,T) >= \sum_i A_i e^{-E_i(R)T}. \tag{1}$$

$E_0(R)$ is of special interest since it contains the static quark potential:

$$E_0(R) = -\frac{\alpha}{R} + \sigma R + \frac{c(\beta)}{a(\beta)}. \tag{2}$$

The term independent of R is the self energy of the two quarks which does not scale but diverges as $a \rightarrow 0$. Since Wilson loops can be calculated quite accurately, the static potential is a useful physical quantity to check scaling and thereby determine the lattice spacing $a(\beta)$. All our data is consistent with standard values $a(2.3) = 0.171$ fm, $a(2.4) = 0.128$ fm and $a(2.5) = 0.089$ fm.

2.2. Flux Tube Profiles

The lattice observable needed to measure the flux is the following[6,1,2].

$$\begin{aligned} f^{\mu\nu}(x) &= \frac{\beta}{a^4}\left(\frac{\langle W P_x^{\mu\nu}\rangle}{\langle W\rangle} - \langle P\rangle\right), \\ &\approx \frac{\beta}{a^4}\left(\frac{\langle W P_x^{\mu\nu} - W P_{x_R}^{\mu\nu}\rangle}{\langle W\rangle}\right), \end{aligned} \tag{3}$$

[2]Haymaker, Singh and Wosiek

where W is the Wilson loop, $P_x^{\mu\nu}$ the plaquette located at x, $\beta = \frac{4}{g^2}$ and x_R is a distant reference point. In the classical continuum limit

$$f^{\mu\nu} \xrightarrow{a\to 0} -\frac{1}{2}\langle (F^{\mu\nu})^2 \rangle_{q\bar{q}-vac}, \tag{4}$$

where the notation $\langle \cdots \rangle_{q\bar{q}-vac}$ means the difference of the average values in the $q\bar{q}$ and vacuum state. From now on we shall be using field components in Minkowski space and hence

$$f^{\mu\nu} \to \frac{1}{2}(-B_1^2, -B_2^2, -B_3^2; E_1^2, E_2^2, E_3^2). \tag{5}$$

Correspondence between various components and $f^{\mu\nu}$ is standard: space-space plaquettes are magnetic, space-time plaquettes are electric. The energy and action densities are respectively

$$\begin{aligned} \epsilon &= \frac{1}{2}(E^2 + B^2), \\ \gamma &= \frac{1}{2}(E^2 - B^2). \end{aligned} \tag{6}$$

Since the magnetic contribution turns out to be negative, there is a strong cancellation between the two terms in the energy, whereas they are enhanced in the action.

Figure 1 gives the flux profiles. The cancellation which suppresses the energy density in the flux tube is evident. However notice that the self energy of the quarks is not similarly suppressed. This follows because the self energy is primarily electric. We fitted the energy and action density in the plane at the midpoint between q and $\bar{q}$ using the function

$$f(r_\perp) = a \exp\Big(-\sqrt{b^2 + (r_\perp/c)^2}\Big). \tag{7}$$

The peak value and the width at half maximum were very well determined using a χ^2 fit for each of 70 cases of different loop sizes and values of β. For the third parameter we chose the decay length of the tail of this function and found it less well determined but with a value typically close to the width at half maximum. The details of the analysis will be given in a forthcoming paper[3]. Here we just give the results of the extrapolation to infinite Wilson loop time extent in Figs. 2 and 3.

The basic issue is whether the peak value of the energy density stabilizes to a constant or goes to zero with quark separation. This is not easy to settle as can be seen in Fig. 2. Roughly speaking we know from the linearly rising potential that the string tension $\sim$ (width)^2 $\times$ (peak value) should be constant. Both Figs. 2 and 3 show that we are marginally asymptotic in quark separation, R. The two curves are $\sim 1/R^4$ and $\sim 1/R$. A Coulomb field would fall like the former but since the string tension is constant the asymptotic width would have to grow like R^2 which clearly it does not. Therefore we can rule out a Coulomb field as expected. Interestingly for small separations, the eyeball fit to $\sim 1/R^4$ is quite good which may be due to a

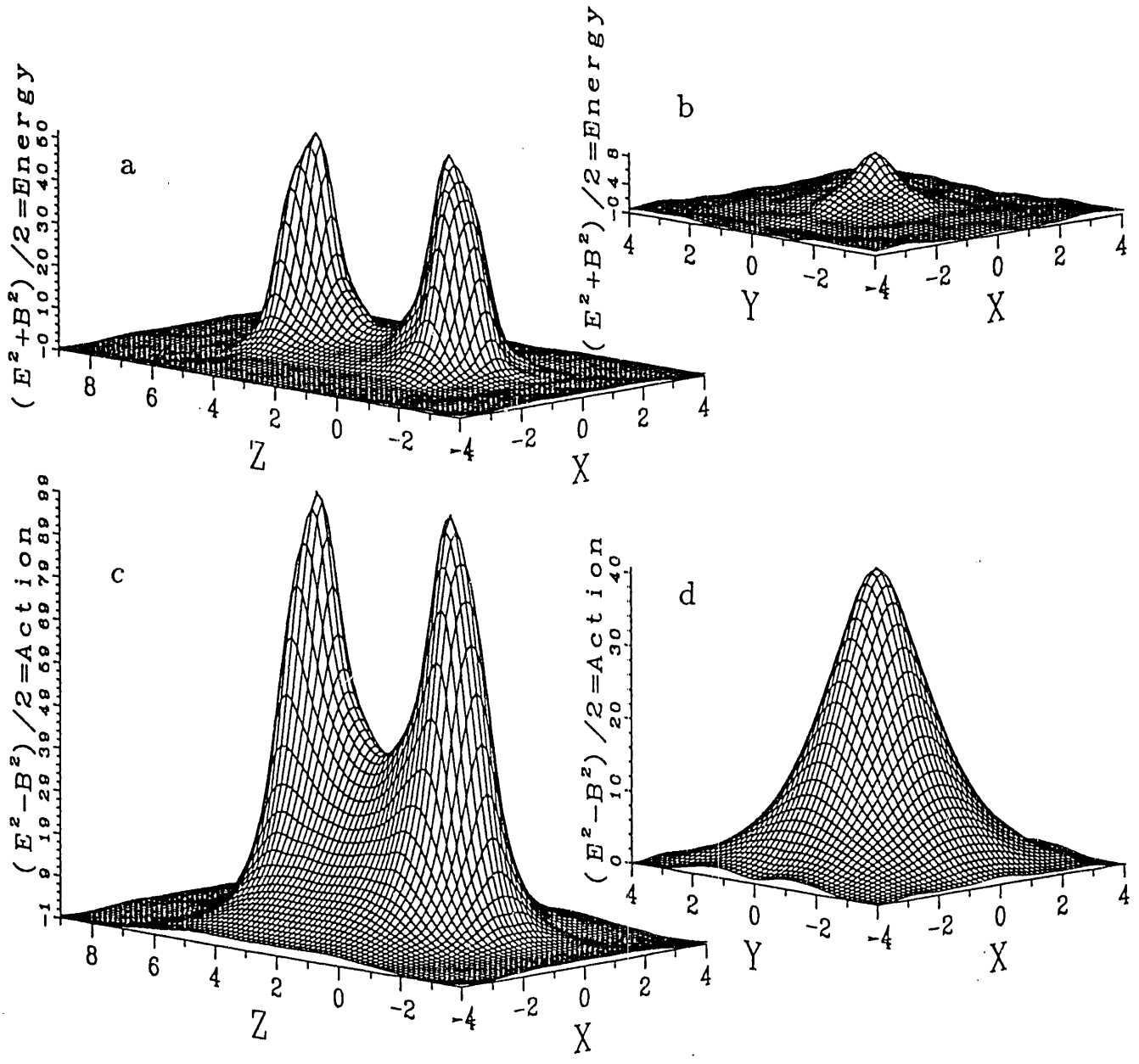

Figure 1: Energy and action profiles: (a) energy density in the plane containing $q\bar{q}$; (b) energy density in the plane midway between q and $\bar{q}$; (c) and (d) similarly for action density.

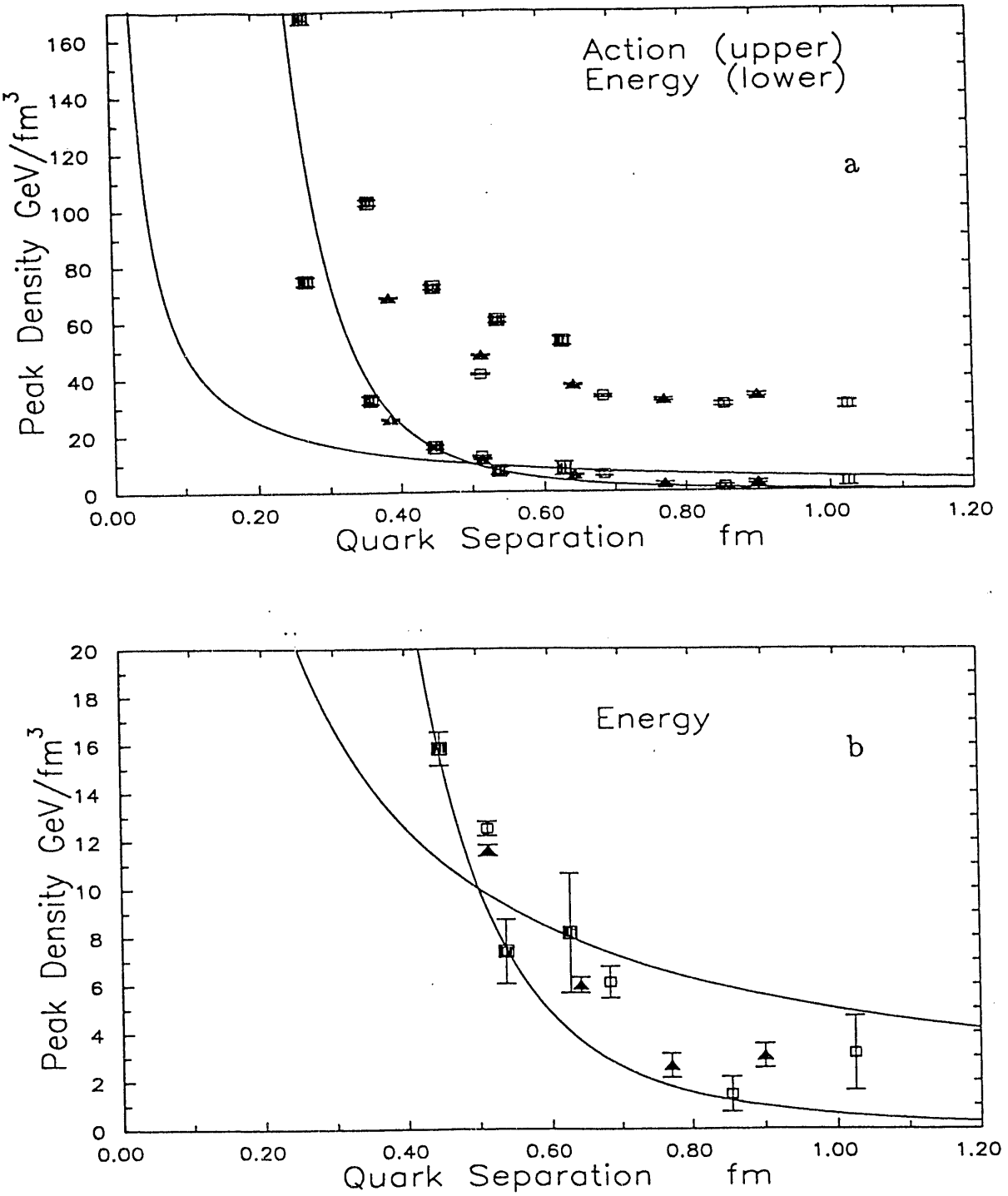

Figure 2: (a) Peak value of energy and action density; solid squares: $\beta = 2.5$; triangles: $\beta = 2.4$; open squares: $\beta = 2.3$. The two curves are $1/R$ and $1/R^4$ arbitrarily normalized; (b) blowup of (a).

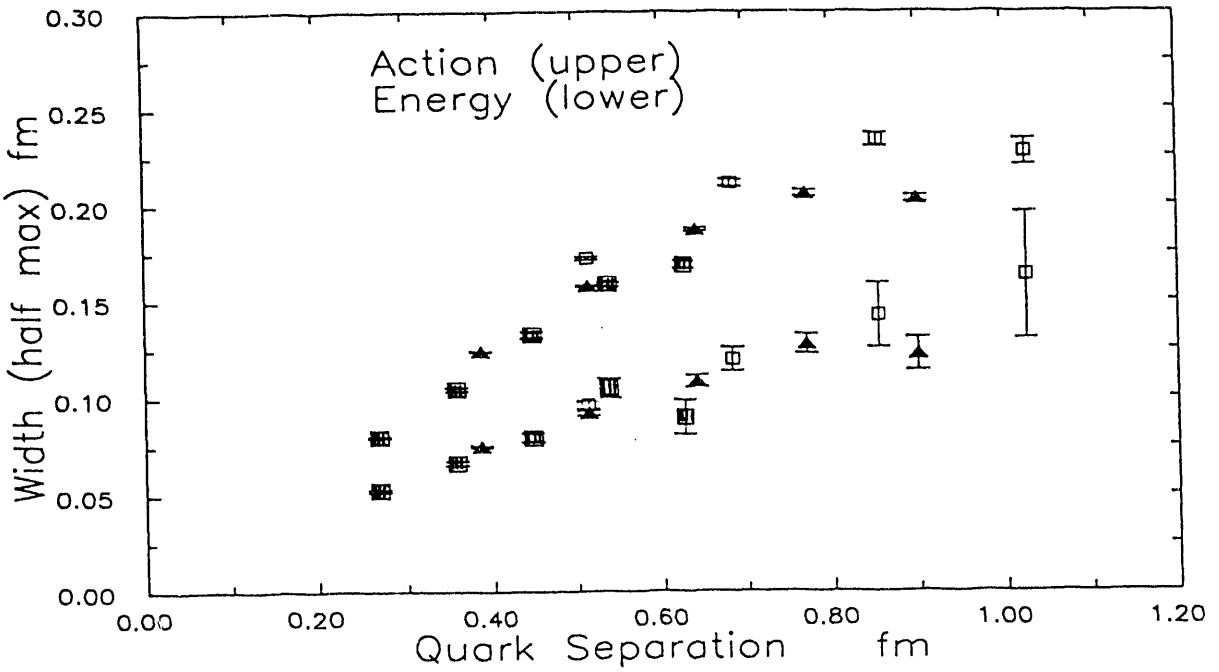

Figure 3: Width at half maximum for energy and action density.

Coulomb like behavior at small distances. (The above argument that the width must grow like R^2 does not apply because there is no string for small R.) The dielectric model[16] predicts the peak density $\sim 1/R$. This function (arbitrarily normalized) does not seem to fit the data very well. However such a behavior would imply the width $\sim \sqrt{R}$ which is certainly possible in our data. We can say that the peak energy density and width are consistent with a constant value for large quark separation but we can not rule out a slow variation. The issue can be tightened by making use of the Michael sum rules[4] as we mention in the next section.

Figure 4 illustrates a general feature of our data. The cluster of three points for each R and T correspond to the three quantities:

$$\begin{aligned} \epsilon &= \frac{1}{2}(E_{\|}^2 + B_{\|}^2) + \frac{1}{2}(E_{\perp}^2 + B_{\perp}^2), \\ \epsilon_{\|} &= \frac{1}{2}(E_{\|}^2 + B_{\|}^2), \\ \epsilon(T \leftrightarrow R) &= \frac{1}{2}(E_{\|}^2 + B_{\|}^2) - \frac{1}{2}(E_{\perp}^2 + B_{\perp}^2). \end{aligned} \tag{8}$$

If one turns the Wilson loop on its side, the $\|$ components are unchanged but the $\perp$ components of the electric and magnetic fields are reversed: $E_{\perp}^2 \leftrightarrow -B_{\perp}^2$. Hence there is a sign change in the third expression. The central points of the cluster are the $\|$ components only. *The clustering of the points implies that the $\perp$ components of the electric and magnetic contributions to energy density are approximately equal but of opposite sign and cancel.* The width of the peak is even less sensitive to the

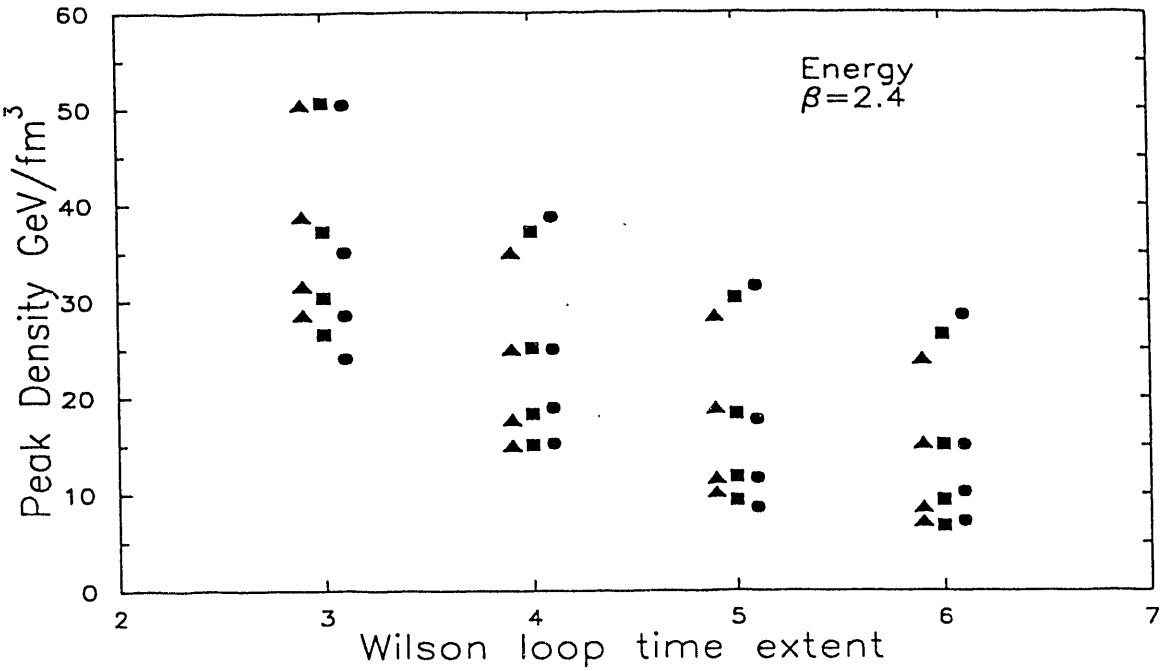

Figure 4: Peak density for $R \times T$ Wilson loop sizes $R = 3-6, T = 3-6$. For fixed T the points decrease monotonically with R. Triangles: energy density for $R \times T$ loop; circles: energy density for $T \times R$ loop; squares: $\|$ components of E^2 and B^2 only.

transverse components giving essentially the same value for all three points.

2.3. Sum Rules

A consistency check on the flux distributions can be obtained by using the Michael sum rules[4] for energy and action.

$$\begin{aligned} \frac{1}{2}\sum_{\vec{x}}(E(\vec{x})^2 + B(\vec{x})^2) &= E_0(R), \\ \frac{1}{2}\sum_{\vec{x}}(E(\vec{x})^2 - B(\vec{x})^2) &= -\beta\frac{\dot{a}}{a}[E_0(R) - \frac{c(\beta)}{a}] - \beta\frac{\dot{c}(\beta)}{a}. \end{aligned} \tag{9}$$

Here $E_0(R)$ is given by Eqn.(1), and $(\cdot \equiv \frac{d}{d\beta})$. In ref.[2] we have shown that our data are essentially consistent with these sum rules. The one difficulty is the fact that the self energy, $c(\beta)/a(\beta)$, determined from the potential differs from the self energy determined from the the action sum rule. This may be due to an ambiguity in the definition of self energy or possibly due to our classical expressions for energy and action which ignores quantum corrections. By taking a derivative of these expressions with respect to the quark separation, R, this difficulty is avoided. This gives the relation

$$\sigma_A = -\beta\frac{\dot{a}}{a}\sigma; \quad \sigma_A \equiv \frac{1}{2}\sum_{\vec{x}_\perp}(E(\vec{x})^2 - B(\vec{x})^2); \quad \sigma \equiv \frac{1}{2}\sum_{\vec{x}_\perp}(E(\vec{x})^2 + B(\vec{x})^2). \tag{10}$$

The sums are now over the plane midway between the $q\bar{q}$ pair.

Using the sum rules we find that the β function $(-\beta\dot{a}/a) \approx 10.\pm 2.$ compared to the current estimates $7.\pm 1.$. The asymptotic value is $-51/121 + 3\pi^2\beta/11 = 6.0(\beta = 2.4)$. There is ample evidence from other measurements that although scaling works well, asymptotic scaling is violated[8] and hence we do not expect to get the asymptotic value.

An alternative approach is to assume the sum rules are correct and use them to infer information about the energy density from the action density which is far easier to measure since relative errors are down by an order of magnitude. As is clear from the sum rule, the action does not scale yet the variation over these values of β is very small. An examination of Fig. 2(a) shows that the action for each β seems to stabilize to a constant for increasing distance for the peak density and for the width. This is quite striking for $\beta = 2.3$ and 2.4. For $\beta = 2.5$ R appears to be too small to draw a conclusion. These data do not suggest that the peak value is tending to zero at all. We would like to use the sum rules to predict the behavior of the energy density. A constant peak energy density follows only if the widths of the energy and action peaks have the same behavior. Figure 3 shows that in fact they do. *From this and using the sum rules we conclude that the energy density stabilizes to a constant value also.* This conclusion is an argument against the dielectric model[16]. However we have little to say about logarithmic behavior of the flux tube width as predicted by Lüscher[7]. For more details see Ref.[3].

3. Mechanism for confinement in U(1)[3]

3.1. Dual Superconductor Model of Confinement

We now turn to the mechanism for flux tube formation and present direct evidence that supercurrents of magnetic monopoles produce a dual Abrikosov vortex[9]. U(1) lattice gauge theory in 4 dimensions has both a confined phase at large charge and a weak coupling deconfined phase corresponding to continuum electrodynamics with a Coulomb interaction between static charges. Therefore confinement or its absence can be studied using U(1) lattice gauge theory as a prototype, before tackling the more complicated non-Abelian theories that actually describe quarks. Much evidence for the dual superconductor hypothesis has accumulated from studies[10,11,12] of lattice gauge theory. Polyakov[10] and Banks, Myerson and Kogut[11] showed that U(1) lattice gauge theory in the presence of a quark-antiquark pair could be approximately transformed into a model describing magnetic current loops (the monopoles) interacting with the electric current generated by the $q\bar{q}$ pair. DeGrand and Toussaint[12] demonstrated via a numerical simulation that the vacuum of U(1) lattice gauge theory was populated by monopole currents, copious in the confined phase and rare in the deconfined phase. This behavior has also been seen in non-Abelian models after gauge fixing[13]. Many studies of non-Abelian models using Dirac monopoles[13,14] or other topological excitations[15] support the dual superconductor mechanism, although other studies[17] dissent.

[3]Singh, Haymaker and Browne

So far, studies of confinement have examined "bulk" properties such as the monopole density[12,13], and the behavior of the static quark potential[14]. In a recent paper[5] we presented the first direct evidence that the flux tube is a dual Abrikosov vortex. We further show that there are exact U(1) lattice gauge theory analogues of two key relations that lead to the Meissner effect in a superconductor; the London equation and the fluxoid quantization condition.

3.2. Electric Field Profiles

Our simulations were done on a Euclidean spacetime lattice of volume $9^3 \times 10$. The static charges are represented by a Wilson loop as in the previous section. We take a 3×3 loop in the $z-t$ plane and measure the fields in the $x-y$ plane at the midpoint between the charges. Because of the geometrical symmetry of the measurements only the z-components of $\langle \vec{\mathcal{E}} \rangle$ and $\langle \vec{\nabla} \times \vec{J}_M \rangle$ are nonzero. If the Wilson loop is removed, even the z-components average to zero, so the response is clearly induced by the presence of the static charges. Only the imaginary part of the Wilson loop contributes to the averages of these two quantities.

The plaquette measures flux passing through a unit square on the lattice[4]

$$\exp[iea^2 F_{\mu\nu}(\vec{r})] = \exp[i\theta_{\mu\nu}(\vec{r})] \equiv U_\mu(\vec{r}) U_\nu(\vec{r}+\mu) U_\mu^\dagger(\vec{r}+\nu) U_\nu^\dagger(\vec{r}). \qquad (11)$$

The electric flux in lattice variables is

$$\mathcal{E}_\mu(\vec{r}) = \mathrm{Im} \exp[i\theta_{\mu 4}(\vec{r})]. \qquad (12)$$

Figure 5(a) shows the electric flux distribution for $\beta = 1.1$ where the vacuum is in the deconfined phase. The broad flux distribution seen is identical to the dipole field produced by placing two classical charges at the quark positions, except that the classical value of the flux on the $q\bar{q}$ axis is a factor of two smaller. We measure the total electric flux from one quark to the other, including not only the flux through the plane between the charges (0.8504 ± 0.0045) but also the flux (0.0951 ± 0.0028) that flows through the lattice boundary because of the periodic boundary conditions. This yields a total flux of (0.9453 ± 0.0053), close to the theoretical value $\Phi_e = e/\sqrt{\hbar c} = 1/\sqrt{\beta} = 0.9534$.

Figure 5(b) and 6(a) shows the electric flux in the confined phase ($\beta = 0.95$). In this case the flux is confined almost entirely within one lattice spacing of the axis and essentially no flux passes the long way around through the lattice boundary. The net flux is again equal to $1/\sqrt{\beta}$ within statistical error. This behavior is exactly what one would expect from the superconducting analogy, where the flux has been "squeezed" into a narrow tube.

3.3. Magnetic Monopole Supercurrents

The monopole currents are found by a prescription devised by DeGrand and Toussaint[12], which employs a lattice version of Gauss' Law to locate the Dirac

[4]The flux here means $E\times$ (area). We use the same term for E^2 or B^2 since it has become an accepted usage.

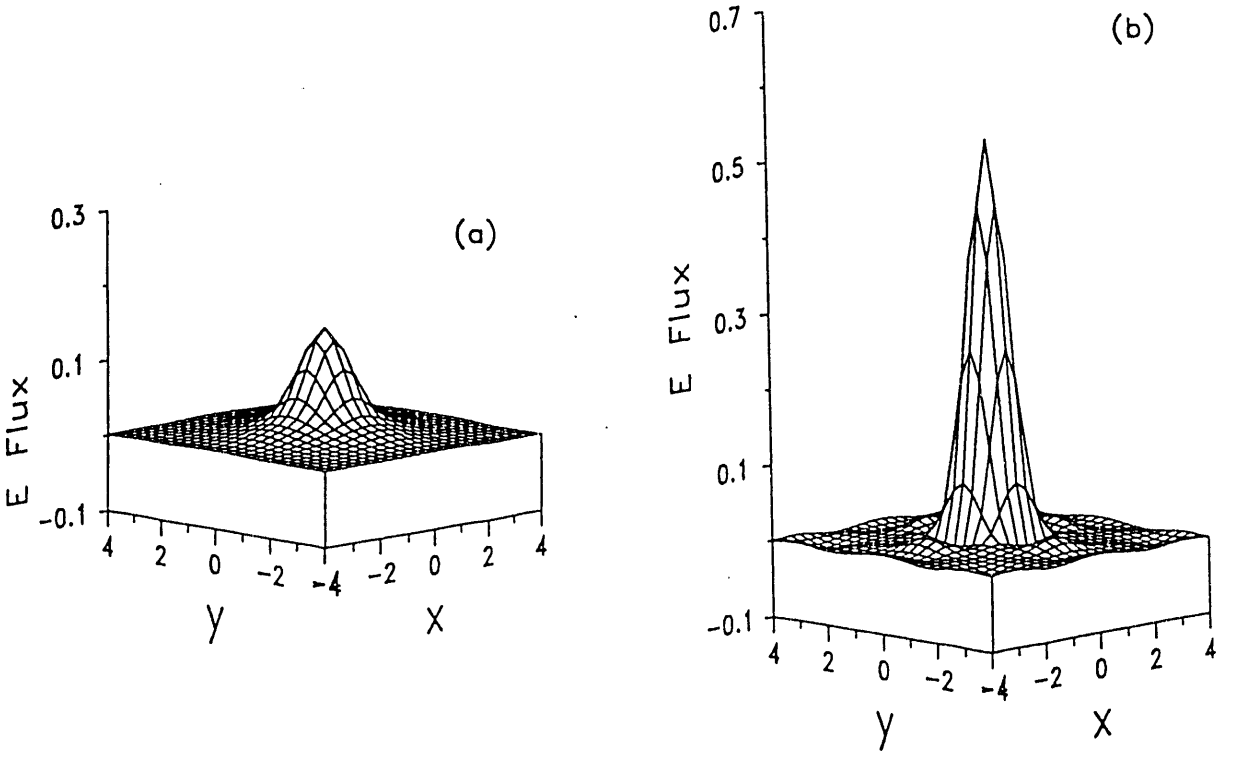

Figure 5: Surface plot of the electric flux through the xy plane midway between the $q\bar{q}$ pair when the system is in (a) the deconfined phase ($\beta = 1.1$) and (b) the confined phase ($\beta = 0.95$). The line joining the pair is located at (0,0).

string attached to the monopole. The net flux into each plaquette face is given by $(\theta_{\mu\nu}(\vec{r}) \bmod 2\pi)$. If the sum of the fluxes into the faces of a 3-volume at fixed time is nonzero, a monopole is located in the box. A non-zero net flux can occur only if a multiple of 2π arises from the mod operation. Therefore the net flux is

$$\sum_{6faces} a^2 F_{\mu\nu} = n(2\pi\hbar c/e) = ne_M \tag{13}$$

The net flux into the box at fixed time thus yields the monopole "charge" density, the time component of the monopole 4-current J_M. The spatial components are found similarly. The monopole currents form closed loops due to the conservation of magnetic charge. Finally the curl is calculated by the line integral of the current around a dual plaquette.

We show in Fig. 6(a) $\langle\vec{\mathcal{E}}\rangle$ and in Fig. 6(b) $-\langle\vec{\nabla}\times\vec{J}_M\rangle$ in the confined phase as a function of the distance from the $q\bar{q}$ axis. The data show that the spatial variation of the flux and the curl of the current are very similar, except for the point on the axis which will be discussed below.

3.4. London Equations, Fluxoid Quantization and the Abrikosov Vortex

In order to interpret this result we would like to review the ordinary London theory. In the next section we interchange electric and magnetic quantities to get the dual results.

A concise statement of the London theory is contained in the relation[5]

$$\vec{A} + \frac{\lambda^2}{c}\vec{J} = 0; \quad (\vec{\nabla} \cdot \vec{A} = 0). \tag{14}$$

If the charge density is zero, then in this gauge the electric field is given by $-\dot{A}/c$ and therefore $\vec{E} = \lambda^2 \dot{\vec{J}}/c$. This describes a perfect conductor and is just Newton's law for free carriers, $e\vec{E} = m\dot{\vec{v}}$. By taking the curl of Eqn.(14) we obtain the condition for a perfect diamagnet.

$$\vec{\nabla} \times \vec{J} = -\frac{c}{\lambda^2}\vec{B}. \tag{15}$$

This relation together with Ampere's law $\vec{\nabla} \times \vec{B} = \vec{J}/c$ gives $\nabla^2\vec{B} = \vec{B}/\lambda^2$ which implies that the magnetic field falls off in the interior of the superconductor with a skin depth λ.

Finally the fluxoid is given by the integral

$$\int_S (\vec{B} + \frac{\lambda^2}{c}\vec{\nabla} \times \vec{J}) \cdot \hat{n} da = \int_C (\vec{A} + \frac{\lambda^2}{c}\vec{J}) \cdot d\vec{l} = n\frac{\hbar c}{2e} = n\Phi_m \tag{16}$$

If the curve C is in a simply connected region of a superconductor, then $n = 0$. However if the curve encircles a hole in the material then n need not be zero but must be an integer. In an extreme type II Abrikosov vortex, a very small core is comprised of normal material. A single unit of magnetic flux of radius $\sim \lambda$ passes through the vortex. The fluxoid density $\vec{B} + \frac{\lambda^2}{c}\vec{\nabla} \times \vec{J}$ is zero everywhere except in the region of the normal material. In the limit in which the core is a delta function we obtain:

$$\vec{B} + \frac{\lambda^2}{c}\vec{\nabla} \times \vec{J} = \Phi_m \delta^2(x_\perp)\hat{n}_z. \tag{17}$$

Further if we use Ampere's law we can get an analytic expression for B_z.

$$B_z(r_\perp) - \lambda^2\nabla^2 B_z = \Phi_m \delta^2(x_\perp); \quad B_z = \frac{\Phi_m}{2\pi\lambda^2} K_0(r_\perp/\lambda). \tag{18}$$

3.5. Dual Superconductor

We interpret our results using the following relations which are the dual of the corrsponding relations in the previous section:

$$\vec{E} - \frac{\lambda^2}{c}\nabla \times \vec{J_m} = \Phi_e \delta^2(x_\perp)\hat{n}_z. \tag{19}$$

where the unit of electric flux $\Phi_e = 1/\sqrt{\beta}$. Figure 5(c) shows the result of fitting our data to this relation. The London penetration depth, λ, is the only free parameter. We are able to determine a value of λ which gives zero away from the axis and a delta

[5]We use Heaviside-Lorentz units to be consistent with lattice gauge theory.

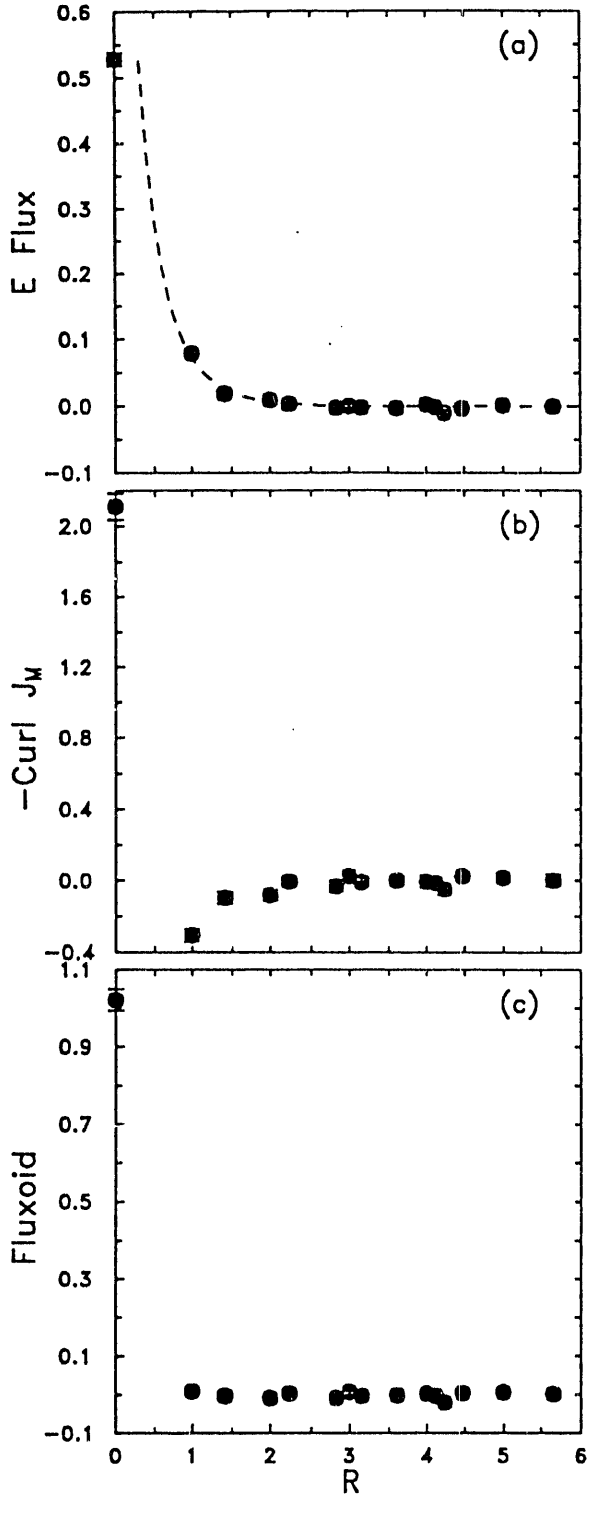

Figure 6: Behavior of (a) the electric flux, (b) the curl of the monopole current and (c) their sum, the fluxoid, in the confined phase ($\beta = 0.95$) as a function of the perpendicular distance $r_\perp$ from the $q\bar{q}$ axis. The solid line in (a) gives the flux for a pure Coulomb field .

unction with the correct coefficient on axis. Further we can check that the electric lux profile is given by

$$E_z = \frac{\Phi_e}{2\pi\lambda^2} K_0(r/\lambda) \tag{20}$$

This function has no free parameters. This curve is also shown in Fig. 6(a) showing excellent agreement. We find a value of $\lambda/a = 0.482 \pm 0.008$, which is consistent with the range of penetration of the electric flux in Fig. 6(a) and the thickness of the current sheet in Fig. 6(b). We expect that, as in a superconductor, the transition to the deconfined phase will be signalled by a divergence of the London penetration depth. We have therefore measured λ further from the deconfinement transition at $\beta = 0.90$, and find a smaller penetration depth of $\lambda/a = 0.32 \pm 0.02$. In the deconfined phase, $\beta = 1.1$ we find an almost insignificant value of $\langle \vec{\nabla} \times \vec{J}_M \rangle$ and fitted values of λ were larger than our lattice size.

In summary, one can find a value of the London penetration depth, λ, that satisfies Eqn.(19) off axis. One then finds that for the point on axis, the same value of λ gives one quantum of electric flux as predicted by Eqn.(19). Finally the same value of λ gives a good fit to the profile using Eqn.(20). Hence considerable detail of the dual Abrikosov is verified. It is perhaps surprising that a nonlinear, strongly interacting, model such as U(1) lattice gauge theory could be described by such a simple model as the linear London equations but our results indicate that the operators $\langle \vec{\mathcal{E}} \rangle$ and $\langle \vec{\nabla} \times \vec{J}_M \rangle$ when measured in the presence of source of external flux like a Wilson loop, give an unambiguous indication of the confinement of electric flux by a monopole current distribution. The simulation yields a large signal even with modesnt amounts of computer time on a Sun workstation. Although the Meissner effect itself requires only that Eq. (20) hold off axis, our data also support the more restrictive fluxoid quantization relation on axis. This additional relation reflects the single-valued nature of the order parameter in a Ginzburg-Landau description of the monopole condensate. Because the monopoles appear pointlike in our simulations, lattice gauge theory looks like an extreme type-II superconductor.

4. Acknowledgements

Two of us (R.W.H. and V.S.) would like to thank A. Kotanski, Y. Peng, G. Schierholz and T. Suzuki for many fruitful discussions on this problem. V.S. thanks A. Kronfeld and R. Wensley for useful conversations. R.W.H and V.S. are supported by the DOE under grant DE-FG05-91ER40617 and D.A.B. is supported in part by the National Science Foundation under Grant No. NSF-DMR-9020310 J.W. is supported in part by the Polish Government under Grants Nos. CPBP 01.01 and CPBP 01.09.

5. References

1. J. Wosiek and R. Haymaker, Phys. Rev. Rapid Commun. D 36, 3297 (1987); J. Wosiek, Nucl. Phys. B (Proc. Suppl.) 4, 52 (1988); R. W. Haymaker and J.

Wosiek, Acta Physica Polonica B 21, 403 (1990). R. W. Haymaker, Y. Peng, V. Singh and J. Wosiek, Nucl.Phys. B (Proc. Suppl.) **17**, 558 (1990).

2. R. W. Haymaker and J. Wosiek, Phys. Rev. D **43**, 2676, (1991)
3. R. W. Haymaker, V. Singh and J. Wosiek, In preparation
4. C. Michael, Nucl. Phys. B **280** [FS18] 13, (1987).
5. V. Singh, R. W. Haymaker, and D. Browne, LSU Preprint LSUHEP - 01 (1992).
6. M. Fukugita and T. Niuya, Phys. Lett. B **132**, 374 (1983); R. Sommer, Nucl. Phys. B **291**, 673 (1987); B **306**, 180 (1988); I. H. Jorysz and C. Michael, Nucl. Phys B **302**, 448 (1987); C. Michael and M. Teper, Nucl. Phys. B **305**, 453 (1988); N. A. Campbell, A. Huntley and C. Michael, Nucl. Phys. B **206**, 51 (1988); S. Perantonis, A. Huntley and C. Michael, Nucl. Phys. **B326**, 544 (1989); W. Feilmair and H. Markum, Nucl. Phys. B **370**, 299 (1992); W. Burger, M. Faber, W. Feilmair, H. Markum and M Muller, Nucl. Phys. **B20** (Proc. Suppl.), 203, (1991);
7. M. Lüscher, Nucl. Phys.B **180** [FS2], 317 (1981); M. Lüscher, G. Münster and P. Weisz, Nucl. Phys. **B180[FS2]**, 1 (1981).
8. C. Michael, Phys. Lett. **B283**, 103, (1992).
9. H. B. Nielsen and P. Olesen, Nucl. Phys. **B61**, 45 (1973); J. Kogut and L. Susskind, Phys. Rev. D 9, 3501 (1974); S. Mandelstam, Phys. Rep. **23C**, 245 (1976); G. 't Hooft, in *High Energy Physics*, ed. A. Zichichi (Editrice Compositori, Bologna, 1976), Nucl. Phys. **B190**[FS3], 455 (1981).
10. A. M. Polyakov, Phys. Lett. **59B**, 82 (1975).
11. T. Banks, R. J. Myerson, and J. Kogut, Nucl. Phys. **B129**, 493 (1977).
12. T. A. DeGrand and D. Toussaint, Phys. Rev. D **22**, 2478 (1980).
13. A. S. Kronfeld, M. L. Laursen, G. Schierholz, and U.-J. Wiese, Phys. Lett. **198B**, 516 (1987); Nucl. Phys. **B293**, 461 (1987); F. Brandstaeter, G. Schierholz, and U.-J. Wiese, Phys. Lett. **272B**, 319 (1991); M. Teper, Phys. Lett. **171B**, 86 (1986); R. J. Wensley and J. D. Stack, Phys. Rev. Lett. **63**, 1764 (1989).
14. T. Suzuki and I. Yotsuyanagi, Phys. Rev. D **42**, 4257 (1990).
15. J. Smit and A. J. van der Sijs, Nucl. Phys. **B355**, 603 (1991); T. L. Ivanenko, A. V. Pochinsky, and M. I. Polikarpov, Phys. Lett. **252B**, 631 (1990).
16. S. L. Adler, Nucl. Phys. B **217**, 381 (1983).
17. J. Greensite and J. Winchester, Phys. Rev. D **40**, 4167 (1989); A. Di Giacomo, M. Maggiore, and S. Olejnik, Nucl. Phys. **B347**, 441 (1990).

DATE
FILMED
02/02/93